The following publication S. -H. Tsang and Y. -L. Chan, "360-Degree Intra Coding Mode for Equirectangular Projection Format Videos," 2020 IEEE International Symposium on Circuits and Systems (ISCAS), 2020, pp. 1-5 is available at https://dx.doi.org/10.1109/ISCAS45731.2020.9180456

# 360-Degree Intra Coding Mode for Equirectangular Projection Format Videos

Sik-Ho Tsang, and Yui-Lam Chan*
Department of Electronic and Information Engineering, The Hong Kong Polytechnic University, Hung Hom, Kowloon, Hong Kong, China
*E-mail: enylchan@polyu.edu.hk

***Abstract*—Recent advances in display, networking, and computing technologies have resulted in changing industry focus towards 360-degree/omnidirectional images as witnessed by increased interest in virtual reality (VR) and augmented reality (AR). Numerous curves are generated for 360-degree images due to the lens curvature and projection format. However, in High Efficiency Video Coding (HEVC), the conventional angular intra modes cannot handle them well since only straight lines can be predicted. More enhanced 360-degree image coding is essential for higher efficiency of storage and transmission. Therefore, we propose a new coding mode, called 360-degree intra mode, for predicting the coding units with curves. Experimental results show that our 360-degree intra mode improves the coding efficiency of HEVC by 0.32% on average and up to 0.74% Bjøntegaard delta bit rate reduction.**

***Keywords—360-degree intra coding, equirectangular projection (ERP), HEVC, omnidirectional, virtual reality***

## I. Introduction

With the facilitation of sensors, computing devices, and 5G networks, it is feasible for the provision of immersive media such as Virtual Reality (VR) and Augmented Reality (AR), which primarily demands 360-degree images. Recently, Motion Picture Experts Group (MPEG) has launched the MPEG-I project for the coding representation of immersive media (ISO/IEC 23090) [1], [2]. It is divided into three phases to support three degrees of freedom (3DoF), 3DoF+, and 6DoF experiences for viewing the immersive media, and they are named as Phase 1a, Phase 1b, and Phase 2, respectively [3]-[5]. In particular, the goal of Phase 1a is to provide users with 3DoF experience of yaw, pitch, and roll for watching 360-degree video content [6]. And MPEG-I has defined the Omnidirectional MediA Format (OMAF) which is the first VR system standard to support 3DoF [7]. As shown in Fig. 1, a 360-degree video, captured by a 360-degree video capture device or generated by multiple stitched images, is projected as a rectangular format followed by encoding. This 360-degree video provides 360×180 degrees of field of view. After transmission and decoding, the video is rendered on the sphere, and a user can view the sphere to experience the 360-degree environment through VR devices such as Head-Mounted Displays (HMDs). Thus, it is essential to improve the coding efficiency of 360-degree images. One of the popular projection formats is equirectangular format (ERP). This format provides one single rectangular image of 360 degrees horizontally and 180 degrees vertically for the ease of encoding. But it also distorts the content and generates many curve based structures within the image.

In High Efficiency Video Coding (HEVC) [8], the conventional HEVC intra mode [9], [10] shown in Fig. 2(a) uses the neighbor boundary pixels to predict a coding unit (CU) with 33 angular predictions plus planar and DC predictions [9]. To reduce the complexity, rough mode decision (RMD) [10] is performed to select a subset of intra prediction candidates first. Then, the optimal one is chosen by rate distortion optimization (RDO) where the full rate distortion (RD) cost for every candidate in the subset is estimated. Planar and DC predictions are used for predicting homogeneous area while 33 angular predictions are used for predicting directional structures with different angles of elevation. However, it is not efficient in numerous specific applications such as depth coding [11]-[13], and screen content coding [14]-[18]. Various new coding tools are invented. Similarly in 360-degree video coding, it cannot efficiently encode the CUs with curves since the conventional angular predictions can only predict straight-line based directional structures, but not CUs that contain curve based structures with different degrees of curvature. An example of ERP image is depicted in Fig. 2. By using the best conventional intra mode among 35 modes, the sum of absolute differences (SAD) in Fig. 2(c) is still much larger than the one in Fig. 2(e) using our proposed 360-degree intra mode, which is elaborated in the following sections. We can also see that our 360-degree intra mode can predict the curve, which can eventually obtain a smaller SAD.

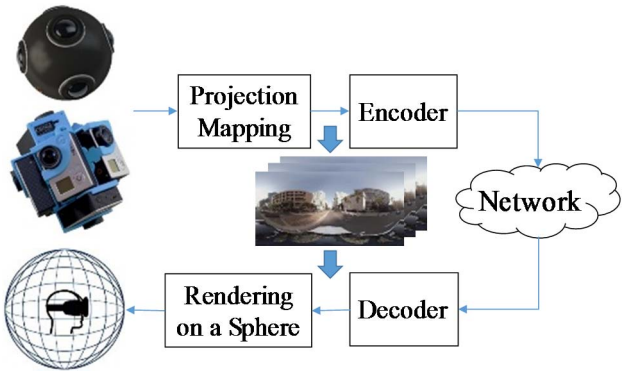


Fig. 1. 360-degree video delivery: from capturing to rendering.


Fig. 2. (a) An example of ERP image, (b)-(c) the prediction and the corresponding residue (lighter color means larger difference) of the conventional intra mode, (d)-(e) the prediction and the corresponding residue (contrast-enhanced) of our proposed 360-degree intra mode.

The work was supported by the Hong Kong Research Grants Council under Research Grant PolyU 152069/18E.

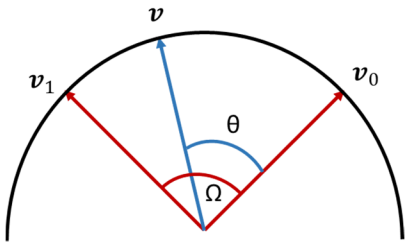


Fig. 3. Illustration of spheric linear interpolation (Slerp).

There are numerous research works to improve coding efficiency of 360-degree video coding. One popular direction is to suggest different kinds of projection mapping in order to reduce the number of pixels per image and improve coding efficiency. Apart from ERP, one widely used projection is cubemap projection (CMP) [19]. There are also icosahedral (ISP) [20], segmented sphere (SSP) [21], adjusted cubemap (ACP) [22], equi-angular cubemap (EAC) [23], and rotated sphere (RSP) [24] projections, etc. Some focus on adaptive downsampling based on the region or latitude [25]-[26]. To the best of our knowledge, there are only a few research works focus on enhancing the coding tools. In [27], RDO in spherical domain is suggested. [28] proposes to pad the reference pixels in intra modes for CUs at the frame border while [29] proposes a regression-based motion vector field for ERP in inter frames.

In this paper, a novel 360-degree intra mode is proposed. Inspired by ***s***pherical ***l***inear int***erp***olation (Slerp), which is originally used in the field of computer graphics, our 360-degree intra mode can predict curves with different degrees of curvature and improve the coding efficiency.

## II. Spherical Linear Int*erp*olation

### A. Linear Interpolation (Lerp)

***L***inear int***erp***olation (Lerp) is to linearly interpolate a vector $\boldsymbol{v}$ according to the given two vectors $\boldsymbol{v_0}$ and $\boldsymbol{v_1}$ as follows:

$$\boldsymbol{v} = (1-t)\boldsymbol{v_0} + t\boldsymbol{v_1} \tag{1}$$

where $t \in [0,1]$. With different values of $t$, we can interpolate a straight line in between $\boldsymbol{v_0}$ and $\boldsymbol{v_1}$.

### B. Spherical Linear Interpolation (Slerp)

In contrast to Lerp, ***s***pherical ***l***inear int***erp***olation (Slerp) in Fig. 3 is to interpolate a curve on a sphere. This is firstly introduced by [30] in the context of quaternion interpolation for the purpose of 3D rotation in computer graphics animation. It is formulated as follows:

$$\boldsymbol{v} = \frac{\sin[(1-t)\Omega]}{\sin\Omega}\boldsymbol{v_0} + \frac{\sin[t\Omega]}{\sin\Omega}\boldsymbol{v_1} \tag{2}$$

where $t \in [0,1]$, $\theta = t\Omega$, and $\Omega$ is the angle between $\boldsymbol{v_0}$ and $\boldsymbol{v_1}$. With different values of $t$, we can interpolate a curve in between $\boldsymbol{v_0}$ and $\boldsymbol{v_1}$. Thereby, by making use of Slerp, we can predict the curved structures generated by ERP in 360-degree images.

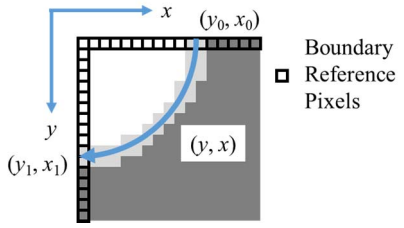


Fig. 4. 360-degree intra coding mode using Slerp.

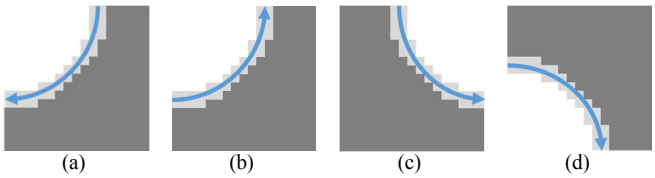


Fig. 5. (a) Top-to-left, (b) left-to-top, (c) top-to-right, and (d) left-to-bottom predictions.

## III. Proposed 360-Degree Intra Coding Mode

### A. Slerp Estimation

Fig. 4 illustrates an example of applying Slerp to have a CU intra prediction. Suppose the vectors in (2) are two dimensional vectors, and with $\theta = t\Omega$, we have:

$$\begin{pmatrix} x \\ y \end{pmatrix} = \frac{\sin(\Omega-\theta)}{\sin\Omega}\begin{pmatrix} x_0 \\ y_0 \end{pmatrix} + \frac{\sin\theta}{\sin\Omega}\begin{pmatrix} x_1 \\ y_1 \end{pmatrix} \tag{3}$$

According to (3), with known ($x_0$, $y_0$) and ($x_1$, $y_1$), the locations of all the points along the curve can be predicted. Suppose ($x_0$, $y_0$) and ($x_1$, $y_1$) are the locations of boundary neighbor pixels at the top and left of the CU respectively, the pixel value of ($x_0$, $y_0$) or ($x_1$, $y_1$) can be assigned to all the points along the curve depending on the prediction direction, i.e.:

$$P(x,y) = P(x_0,y_0) \text{ or } P(x,y) = P(x_1,y_1) \tag{4}$$

where $P(x, y)$ is the pixel value at location $(x, y)$.

However, the pixels inside the CU are at integer-pel locations. Thus, to assign a pixel value to an integer-pel location, at least two location points near to that integer-pel location are estimated. Then, linear interpolation is performed for the pixel value. To do this, suppose $x$ is a known integer, to find the corresponding $y$, $\theta$ is required to be found. By using (3) and consider $y$ first, we obtain:

$$y\sin\Omega = y_0 sin\,\Omega\cos\theta + (y_1 - y_0\cos\Omega)\sin\theta \tag{5}$$

Based on the trigonometric identity of $a\cos\varphi + b\sin\varphi = \sqrt{a^2+b^2}\sin(\varphi + \tan^{-1}a/b)$, (5) is formulated as below:

$$\begin{aligned} y\sin\Omega = {} & \sqrt{(y_0\sin\Omega)^2 + (y_1 - y_0\cos\Omega)^2} \\ & \times \sin\left(\theta + \tan^{-1}\frac{y_0\sin\Omega}{y_1 - y_0\cos\Omega}\right) \end{aligned} \tag{6}$$

And based on (6), $\theta$ can be estimated as follows:

$$\theta = \sin^{-1}\left(\frac{y\sin\Omega}{\sqrt{(y_0\sin\Omega)^2 + (y_1 - y_0\cos\Omega)^2}}\right) - \tan^{-1}\frac{y_0\sin\Omega}{y_1 - y_0\cos\Omega} \tag{7}$$

With known $\theta$, we can obtain $x$ using (3) with the corresponding integer $y$. Therefore, by looping the pairs of ($x_0$, $y_0$) and ($x_1$, $y_1$), which are the locations of boundary neighbor

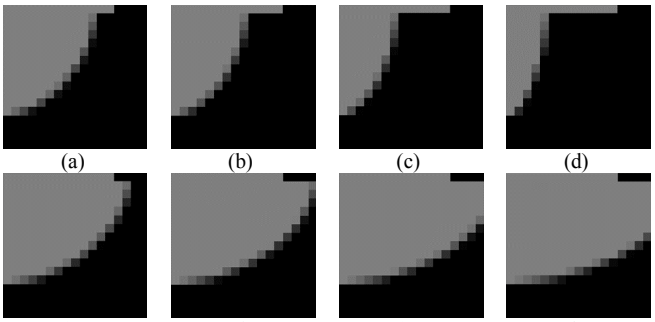

Fig. 6. (a) $\Delta x$=2, (b) $\Delta x$=4, (c) $\Delta x$=6, (d) $\Delta x$=8, (e) $\Delta y$=2, (f) $\Delta y$=4, (g) $\Delta y$=6, and (h) $\Delta y$=8 for left-to-top predictions.

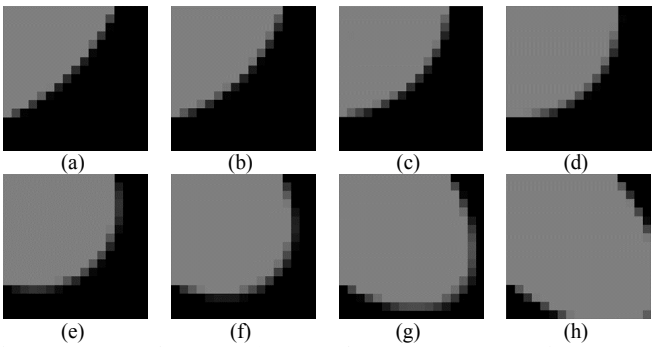

Fig. 7. (a) $\Omega$=70, (b) $\Omega$=80, (c) $\Omega$=90, (d) $\Omega$=100, (e) $\Omega$=110, (f) $\Omega$=120, (g) $\Omega$=130, and (h) $\Omega$=140 for left-to-top predictions ($\Delta x$=$\Delta y$=0).

pixels at the top and left of the CU respectively, for each pixel location within the CU, the two nearest locations, one from the left, $(x_L, y_L)$, and one from the right, $(x_R, y_R)$, can be found. Once the two nearest locations can be found, the pixel value is then linearly interpolated by the corresponding pixel values of those two nearest locations, i.e.:

$$P(x_i, y_j) = D_R \cdot P(x_L, y_L) + D_L \cdot P(x_R, y_R)/(D_L + D_R) \quad (8)$$

where $D_L$ and $D_R$ are the distances of $(x_L, y_L)$ and $(x_R, y_R)$ with the current integer-pel location $(x_i, y_j)$ within the CU respectively.

### B. 360-Degree Intra Mode Parameters

Since the representations of a curve are much complicated than a straight line, several coding parameters for our proposed 360-degree intra mode are required instead of only the intra prediction direction for the conventional intra mode.

First, there are four *prediction directions* supported in our proposed 360-degree intra coding mode, namely top-to-left, left-to-top, top-to-right, and left-to-bottom predictions as shown in Fig. 5. And there is no right-to-bottom or bottom-to-right prediction due to the absence of reference pixels.

In Fig. 5, for the pair of boundary neighbor locations $(x_0, y_0)$ and $(x_1, y_1)$, $x_0 = y_1$. Thereby, only circular curves are generated. To generate curves with different degrees of curvature, the pair of boundary neighbor locations can be changed to $(x_0+\Delta x, y_0)$ and $(x_1, y_1)$, or $(x_0, y_0)$ and $(x_1, y_1+\Delta y)$. Thus, *an offset flag* is to indicate whether $\Delta x$ or $\Delta y$ is used and *an offset* is to indicate the size of $\Delta x$ or $\Delta y$. Fig. 6 depicts the cases when $\Delta x$ is non-zero ((a)-(d)) and $\Delta y$ is non-zero ((e)-(h)) for left-to-top prediction. It is noted that $\Delta x$=$\Delta y$=0 for the cases in Fig. 5.

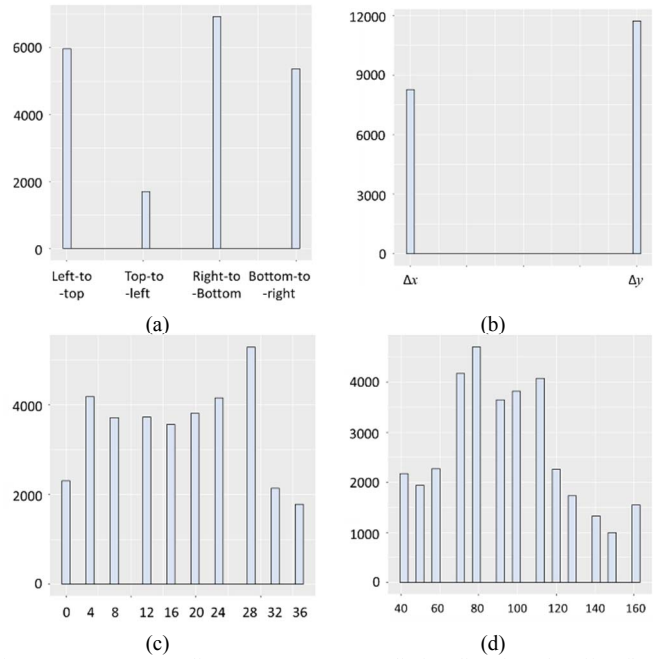


Fig. 8. Statistics of coding parameters: (a) prediction direction, (b) offset flag, (c) offset, and (d) angle.

Lastly, there is also *an angle parameter* to determine the value of $\Omega$ in (3). With different values of $\Omega$, more curved structures can be generated as depicted in Fig. 7. It is noted that $\Omega$=90 for the cases in Fig. 5 and Fig. 6. As seen from the figure, when $\Omega$ is too small, the curve generated is similar to a straight line which can be efficiently predicted by the conventional intra angular prediction. When $\Omega$ is too large, the curve generated is bended severely which may not be the cases in ERP.

With fine-grained parameters, more bits are needed for the curve representation which will increase the coding bits of the mode. On the other hand, with coarse-grained parameters, prediction is not accurate enough which will increase the SAD of the mode. Hence, the selection of parameters to be coded is carefully studied in the coming sub-section.

### C. Selection of Parameters

As mentioned, there are four sets of parameters needed to be coded for our proposed 360-degree intra mode: prediction direction, offset, offset flag, and angle. We randomly selected ten ERP images from Salient360! dataset [31] for testing the selection of parameters. To test the effectiveness, the parameters of the best 360-degree intra mode are recorded if our proposed mode has smaller SAD than the best conventional intra mode.

Fig. 8 depicts the frequency counts of the four sets of parameters. For prediction direction, though top-to-left prediction has fewer counts than others, it is decided to have four directions which needs two-bit signaling. For offset flag, one-bit signaling is used. For the offset coding, it is decided to have three-bit signaling to represent the first eight offsets. This is because when the offsets are too large, it becomes a straight line which can be efficiently encoded by the conventional intra mode. For the angle coding, it is decided to have two to three-bit signaling to represent 70-degree to 120-degree angles with steps of 10 since if it is too small, it becomes a straight line which can be efficiently encoded by the conventional intra mode.

TABLE I. BD-RATE (%) USING WS-PSNR AND S-PSNR OF OUR PROPOSED 360-DEGREE INTRA MODE AGAINST THE CONVENTIONAL HEVC

| BD-rate | Using WS-PSNR (%) | | | Using S-PSNR (%) | | |
|---|---|---|---|---|---|---|
| Enabled at | CU64 | CU32 | CU64 +CU32 | CU64 | CU32 | CU64 +CU32 |
| P2 | -0.03 | -0.03 | -0.27 | -0.09 | -0.30 | -0.32 |
| P4 | -0.03 | -0.03 | -0.18 | -0.01 | -0.22 | -0.30 |
| P5 | -0.04 | -0.04 | -0.24 | 0.00 | -0.27 | -0.18 |
| P6 | 0.01 | 0.01 | -0.36 | 0.04 | -0.17 | -0.38 |
| P12 | -0.01 | -0.01 | -0.03 | 0.02 | -0.03 | -0.02 |
| P15 | 0.04 | 0.04 | -0.53 | 0.10 | -0.57 | -0.58 |
| P17 | -0.03 | -0.03 | -0.58 | -0.04 | -0.64 | -0.45 |
| P21 | -0.07 | -0.07 | -0.39 | -0.14 | -0.34 | -0.55 |
| P23 | -0.01 | -0.01 | -0.52 | 0.02 | -0.62 | -0.59 |
| P25 | 0.02 | 0.02 | -0.19 | 0.00 | -0.20 | -0.33 |
| P27 | -0.06 | -0.67 | **-0.71** | -0.14 | -0.72 | **-0.74** |
| P31 | -0.02 | -0.36 | -0.39 | 0.02 | -0.38 | -0.42 |
| P35 | 0.02 | -0.24 | -0.18 | 0.03 | -0.21 | -0.32 |
| P45 | 0.05 | -0.13 | -0.19 | 0.01 | -0.12 | -0.26 |
| P47 | 0.02 | -0.10 | -0.08 | -0.08 | -0.10 | -0.13 |
| P49 | 0.01 | -0.37 | -0.40 | -0.10 | -0.43 | -0.42 |
| P55 | 0.01 | -0.13 | -0.08 | 0.06 | -0.12 | -0.16 |
| P62 | -0.04 | -0.12 | -0.13 | -0.14 | -0.15 | -0.22 |
| P63 | -0.03 | -0.05 | -0.03 | -0.08 | -0.09 | -0.21 |
| P66 | -0.11 | -0.22 | -0.27 | -0.09 | -0.29 | -0.19 |
| P68 | 0.04 | -0.13 | -0.08 | 0.07 | -0.11 | -0.05 |
| P84 | 0.00 | -0.20 | -0.20 | 0.02 | -0.18 | -0.15 |
| P87 | 0.14 | -0.25 | -0.23 | -0.06 | -0.47 | -0.56 |
| P88 | 0.02 | -0.21 | -0.18 | -0.13 | -0.42 | -0.40 |
| P89 | -0.02 | -0.05 | -0.05 | -0.14 | -0.16 | -0.17 |
| **Average** | -0.01 | -0.14 | **-0.26** | -0.03 | -0.29 | **-0.32** |
| **Top 10** | -0.05 | -0.28 | **-0.42** | -0.04 | -0.43 | **-0.44** |

### D. HEVC Implementation

As aforementioned in the previous sub-section, there are four types of prediction directions, two choices for the offset flag, eight offsets, and six angle parameters. The total combination for RD cost estimation is 4×2×8×6=384, which is ten times more than the conventional intra mode of 35 combinations. To limit the computational complexity, similar to the conventional intra mode, RMD [10] is also performed in our proposed 360-degree intra mode. The sum of absolute transformed differences (SATD) is estimated for each mode candidate first. Only the nine candidates with the smallest SATD is selected for full RDO estimation. And our proposed 360-degree intra mode is only used in large-size CUs, i.e. CU 64×64 and CU 32×32 since the conventional intra mode is already efficient enough for coding small-size CUs.

In addition to the above parameters, there is also a CU-level one-bit signaling flag to indicate the use of our proposed 360-degree intra mode. Thus, the 360-degree intra mode competes using RDO with the conventional intra mode at CU level. For CUs that are at the frame boundary, 360-degree intra mode is disabled due to the lack of boundary reference pixels.

## IV. EXPERIMENTAL RESULTS

To evaluate the performance of the proposed 360-degree intra coding mode, we performed experiments on 25 ERP images from Salient360! dataset [31] using all-intra configuration according to the common test condition [32]. The HEVC reference software HM-18.16 [33] with the 360-degree reference software package 360Lib-5.0 [34] is used. Since our improvement is within the encoder, Bjøntegaard delta bit rate (BD-rate) [35] is measured using codec-level weighted-to-spherically-uniform PSNR (WS-PSNR) [36] and spherical PSNR (S-PSNR) [37] metrics for objective evaluation [38].

(a) (b)

Fig. 9. Results of ERP images: (a) P12 with 0.03%, and (b) P49 with 0.48% of BD-rate reduction using WS-PSNR respectively.

TABLE I. tabulates the BD-rate (%) using WS-PSNR and S-PSNR of our proposed 360-degree intra mode against the conventional HEVC. It can be seen that with our 360-degree intra mode enabled only at CU 64×64 or CU 32×32, 0.01% and 0.14% average BD-rate reduction using WS-PSNR are obtained respectively. With our 360-degree intra mode enabled at both CU 64×64 and CU 32×32, 0.26% and 0.32% average BD-rate reduction using WS-PSNR and S-PSNR are obtained respectively. As some of the ERP images only obtain very few curved structures and with large portions of plain background such as sky, or irregular shapes like rocks, BD-rate is only reduced in a very small amount or even increased due to the use of CU-level 360-degree intra mode flag. This fact can be shown in Fig. 9. If the top ten images with the largest BD-rate reduction are considered, 0.42% and 0.44% average BD-rate reduction using WS-PSNR and S-PSNR are achieved. For image P27 (Fig. 2(a)), the largest BD-rate reduction using WS-PSNR and S-PSNR of 0.71% and 0.74% are achieved. It is noted that the improvement is already substantial with our proposed 360-degree intra mode only enabled at large-size CUs and only applied on curved structures.

## V. CONCLUSIONS

Conventional video coding tools are not optimal for compressing 360-degree contents since there are many curved structures. In this paper, inspired by Slerp, which is originally used in computer graphics animation, our proposed 360-degree intra mode can efficiently encode those curved structures. With our novel coding mode and carefully selected coding parameters, the coding efficiency is improved with 0.32% on average and up to 0.74% BD-rate reduction using S-PSNR. In the future, further works can be considered to boost the coding efficiency, such as decoder-side approaches, like [39]-[41], can be used to derive the coding parameters in order to reduce the overhead bits of our proposed 360-degree intra mode.

## REFERENCES


[1] R. Skupin, Y. Sanchez, Y.-K. Wang, M. M. Hannuksela, J. Boyce, and M. Wien, "Standardization Status of 360 Degree Video Coding and Delivery," *Proc. IEEE Visual Comm. Image Process. (VCIP)*, pp. 1-4, St. Petersburg, Florida, U.S.A., Dec. 2017.

[2] M. Domański, O. Stankiewicz, K. Wegner, and T. Grajek, "Immersive Visual Media — MPEG-I: 360 Video, Virtual Navigation and Beyond," *Proc. Int. Conf. Syst. Signals Image Process. (IWSSIP)*, pp. 1-9, Poznan, Poland, May 2017.

[3] Y.-L. Chan, C.-H. Fu, H. Chen, and S.-H. Tsang, "Overview of Current Development in Depth Map Coding of 3D Video and its Future," *IET Signal Processing*, eFirst Article, pp. 1-17, Oct. 2019.

[4] S.-H. Tsang, Y.-L. Chan, and W. Kuang, "Standard Compliant Light Field Lenslet Image Coding Model Using Enhanced Screen Content Coding Framework," *J. Electron. Imaging*, vol. 28, no. 5, 053027, pp. 1-12, Oct. 2019.

[5] S.-H. Tsang, Y.-L. Chan, and W. Kuang, "Standard-Compliant HEVC Screen Content Coding for Raw Light Field Image Coding," Accepted, To Be Appeared, *Proc. Int. Conf. Signal Process. Commun. Syst. (ICSPCS)*, pp.1-6, Surfers Paradise, Gold Coast, Australia, Dec. 2019.

[6] "How OMAF Fulfils MPEG-I Phase 1a Requirements," *MPEG*, document N17372, Gwangju, South Korea, Jan. 2018.

[7] M. M. Hannuksela, Y. Wang, and A. Hourunranta, "An Overview of the OMAF Standard for 360-degree Video," *Proc. Data Compression Conf. (DCC)*, pp. 418-427, Snowbird, Utah, U.S.A., Mar. 2019.

[8] G. J. Sullvian, J. Ohm,W. J. Han, and T.Wiegand, "Overview of the High Efficiency Video Coding (HEVC) Standard," *IEEE Trans. Circuits Syst. Video Technol.*, vol. 22, no. 12, pp. 1649–1668, Dec. 2012.

[9] J. Lainema, F. Bossen, W. J. Han, J. Min, and K. Ugur, "Intra Coding of the HEVC Standard," *IEEE Trans. Circuits Syst. Video Technol.*, vol. 22, no. 12, pp. 1792-1801, Dec. 2012.

[10] L. Zhao, L. Zhang, S. Ma, and D. Zhao, "Fast Mode Decision Algorithm for Intra Prediction in HEVC," *Proc. IEEE Visual Comm. Image Process. (VCIP)*, pp. 1-4, Tainan, Taiwan, Nov. 2011.

[11] C.-H. Fu, H. Chen, Y.-L. Chan, S.-H. Tsang, and X. Zhu, "Early Termination for Fast Intra Mode Decision in Depth Map Coding using DIS-inheritance," *J. Signal Process.: Image Commun.*, vol. 80, 115644, pp. 1-9, Feb. 2020.

[12] C.-H. Fu, H. Chen, Y.-L. Chan, S.-H. Tsang, H. Hong, and X. Zhu, "Fast Depth Intra Coding based on Decision Tree in 3D-HEVC," IEEE Access, vol. 7, pp. 173138-173147, Dec. 2019.

[13] H.-B. Zhang, C.-H. Fu, Y.-L. Chan, S.-H. Tsang, and W.-C. Siu, "Probability-based Depth Intra Mode Skipping Strategy and Novel VSO Metric for DMM Decision in 3D-HEVC *IEEE Trans. Circuits Syst. Video Technol.*, vol. 28, no. 2, pp. 513-527, Feb. 2018.

[14] W. Kuang, Y.-L. Chan, S.-H. Tsang, and W.-C. Siu, "Online-Learning-Based Bayesian Decision Rule for Fast Intra Mode and CU Partitioning Algorithm in HEVC Screen Content Coding," *IEEE Trans. Image Process.*, vol. 29, no. 1, pp. 170-185, Jan. 2020.

[15] S.-H. Tsang, Y.-L. Chan and W. Kuang, "Mode Skipping for HEVC Screen Content Coding via Random Forest," *IEEE Trans. Multimedia*, vol. 21, no. 10, pp. 2433-2446, Oct. 2019.

[16] W. Kuang, Y.-L. Chan, S.-H. Tsang, and W.-C. Siu, "DeepSCC: Deep Learning Based Fast Prediction Network for Screen Content Coding," *IEEE Trans. Circuits Syst. Video Technol.*, Early Access Article, pp. 1-15, Jul. 2019.

[17] S.-H. Tsang, Y.-L. Chan, W. Kuang, and W.-C. Siu, "Reduced-Complexity Intra Block Copy (IntraBC) Mode with Early CU Splitting and Pruning for HEVC Screen Content Coding," *IEEE Trans. Multimedia*, vol. 21, no. 2, pp. 269-283, Feb. 2019.

[18] W. Kuang, Y.-L. Chan, S.-H. Tsang, and W.-C. Siu, "Fast Intraprediction for High-Efficiency Video Coding Screen Content Coding by Content Analysis and Dynamic Thresholding," *J. Electron. Imaging*, vol. 27, no. 5, 053029, pp. 1-18, Oct. 2018.

[19] K.T. Ng, S.C. Chan, and H.Y. Shum, "Data Compression and Transmission Aspects of Panoramic Videos," *IEEE Trans. Circuits Syst. Video Technol.*, vol. 15, no. 1, pp. 82–95, Jan. 2005.

[20] V. Zakharchenko, E. Alshina, K. P. Choi, A. Singh, and A. Dsouza, "AhG8: Icosahedral Projection for 360-Degree Video Content," *JVET*, document JVET-D0028, Chengdu, China, Oct. 2016.

[21] J. Li, Z. Wen, S. Li, Y. Zhao, B. Guo, and J. Wen, "Novel Tile Segmentation Scheme for Omnidirectional Video," *Proc. IEEE Int. Conf. Image Process. (ICIP)*, pp. 370-374, Phoenix, Arizona, U.S.A., Sep. 2016.

[22] M. Coban, G. Van der Auwera, and M. Karczewicz, "AHG8: Adjusted Cubemap Projection for 360-Degree Video," *JVET*, document JVET-F0025, Hobart, Australia, Apr. 2017.

[23] Equi-Angular Cubemap. [Online]. Available: https://www.blog.google/products/google-vr/bringing-pixels-front-and-center-vr-video/

[24] A. Abbas, D. Newman, S. N. Akula, and A. Konda, "Next Generation Video Coding for Spherical Content," *Proc. Picture Coding Symp. (PCS)*, pp. 333-336, San Francisco, California, U.S.A., Jun. 2018.

[25] R. G. Youvalari, A. Aminlou, and M. M. Hannuksela, "Analysis of Regional Down-sampling Methods for Coding of Omnidirectional Video," *Proc. Picture Coding Symp. (PCS)*, pp. 1-5, Nuremberg, Germany, Dec. 2016.

[26] S.-H. Lee, S.-T. Kim, E. Yip, B.-D. Choi, J. Song and S.-J. Ko, "Omnidirectional Video Coding Using Latitude Adaptive Down-sampling and Pixel Rearrangement," *IET Electron. Lett.*, vol. 53, no. 10, pp. 655-657, May 2017.

[27] Y. Li, J. Xu and Z. Chen, "Spherical Domain Rate-Distortion Optimization for Omnidirectional Video Coding," *IEEE Trans. Circuits Syst. Video Technol.*, vol. 29, no. 6, pp. 1767-1780, Jun. 2019.

[28] N. Li, S. Wan, and F. Yang, "Reference Samples Padding for Intra-Frame Coding of Omnidirectional Video," *Proc. Asia-Pacific Signal Info. Process. Assoc. Annu. Summit Conf. (APSIPA ASC)*, pp. 1987-1990, Honolulu, HawaiI, U.S.A., Nov. 2018.

[29] R. Ghaznavi-Youvalari, A. Aminlou and J. Lainema, "Regression-based Motion Vector Field for Video Coding," *IEEE Trans. Circuits Syst. Video Technol.*, Early Access Article, pp. 1-6, Sep. 2019.

[30] K. Shoemake, "Animating Rotation with Quaternion Curves," *Proc. Annu. Conf. Comp. Graph. Interacitve Tech. (ACM SIGGRAPH)*, vol. 13, no. 3, pp. 245-254, Jul. 1985.

[31] J. Gutiérrez, E. David, A. Coutrot, M. Perreira Da Silva, and P. Le Callet, "Introducing UN Salient360! Benchmark: A Platform for Evaluating Visual Attention Models for 360 Contents", *Proc. Int. Conf. Quality Multimedia Experience (QoMEX)*, pp. 1-3, Sardinia, Italy, May-Jun. 2018.

[32] "JVET Common Test Conditions and Evaluation Procedures for 360° Video," *JVET*, document JVET-H1030, Macao, China, Oct. 2017.

[33] HEVC Test Model Version HM-16.18 [Online]. Available: https://hevc.hhi.fraunhofer.de/svn/svn_HEVCSoftware/tags/HM-16.18/.

[34] "Algorithm Descriptions of Projection Format Conversion and Video Quality Metrics in 360Lib Version 5," *JVET*, document JVET-H1004, Macao, China, Oct. 2017.

[35] G. Bjøntegaard, "Calculation of Average PSNR Differences Between RD Curves", *VCEG*, document VCEG-M33, Austin, Texas, U.S.A., Mar. 2001.

[36] Y. Sun, A. Lu and L. Yu, "Weighted-to-Spherically-Uniform Quality Evaluation for Omnidirectional Video," *IEEE Signal Process. Lett.*, vol. 24, no. 9, pp. 1408-1412, Sep. 2017.

[37] M. Yu, H. Lakshman, and B. Girod, "A Framework to Evaluate Omnidirectional Video Coding Schemes", *Proc. IEEE Int. Symp. Mixed Augmented Real. (ISMAR)*, pp. 31-36, Fukuoka, Japan, Sep. 2015.

[38] P. Hanhart, Y. He, Y. Ye, J. Boyce, Z. Deng and L. Xu, "360-Degree Video Quality Evaluation," *Proc. Picture Coding Symp. (PCS)*, pp. 328-332, San Francisco, California, U.S.A., Jun. 2018.

[39] S.-H. Tsang, W. Kuang, Y.-L. Chan, and W.-C. Siu, "Decoder Side Merge Mode and AMVP in HEVC Screen Content Coding," *Proc. IEEE Int. Conf. Image Process. (ICIP)*, pp.260-264, Beijing, China, Sep. 2017.

[40] S.-H. Tsang, Y.-L. Chan, and W.-C. Siu, "Fast and Efficient Intra Coding Techniques for Smooth Regions in Screen Content Coding Based on Boundary Prediction Samples," *Proc. IEEE Int. Conf. Acoustics, Speech Signal Process. (ICASSP)*, pp.1409-1413, Brisbane, Australia, Apr. 2015.

[41] S.-H. Tsang, Y.-L. Chan, and W.-C. Siu, "Efficient Intra Prediction Algorithm for Smooth Regions in Depth Coding", *IET Electron. Lett.*, vol. 48, no. 18, pp. 1117-1119, Aug. 2012.